Biomass Conversion and Biorefinery (2018) 8:379–395
https://doi.org/10.1007/s13399-017-0293-3

ORIGINAL ARTICLE

Assessment of zeolite 13X and Lewatit® VP OC 1065 for application in a continuous temperature swing adsorption process for biogas upgrading

Elisabeth Sonnleitner[1] · Gerhard Schöny[1] · Hermann Hofbauer[1]

Received: 19 July 2017 / Revised: 20 July 2017 / Accepted: 2 November 2017 / Published online: 25 November 2017

Abstract
Two commercially available CO_2-adsorbent materials (i.e., zeolite 13X (13X) and Lewatit® VP OC 1065 (Lewatit)) were evaluated for their applicability in a continuous temperature swing adsorption (TSA) process for biogas upgrading. The equilibrium adsorption characteristics of carbon dioxide and methane were determined by fixed bed and TGA tests. While relatively high CO_2 capacities were measured for both materials (3.6 and 2.5 mol kg^{-1}), neither of them was found to adsorb significant amounts of CH_4. Lewatit showed to be fully regenerable at 95 °C, whereas for 13X, the regeneration was not complete at this temperature. However, 13X showed no degradation up to 190 °C, whereas Lewatit started to degrade at 110 and 90 °C when exposed to N_2 and air, respectively. Fluidization tests showed that Lewatit provides a high mechanical stability, while on the contrary, the tested 13X showed considerable attrition. An equilibrium adsorption model was fitted to the measured CO_2 adsorption data. The adsorption model was then integrated into an existing simulation tool for the proposed TSA process to roughly estimate the expectable regeneration energy demand for both materials. It was found that depending on the operating conditions, the regeneration energy demand lies between 0.32–0.54 $kWh_{th}/m^3_{prodgas}$ for 13X and 0.71–1.10 $kWh_{th}/m^3_{prodgas}$ for Lewatit. Since heat integration measures were not considered in the simulations, it was concluded that the proposed TSA process has a great potential to reduce the overall energy demand for biogas upgrading and that both tested adsorbent materials may be suitable for application in the proposed TSA process.

Keywords Biogas upgrading · CO_2 capture · TSA · Solid sorbents

1 Introduction

Biogas is a promising renewable energy source that is considered as carbon neutral since the contained carbon comes from organic matter [1]. It can either be used for power and heat production or preferably sent to an upgrading process to yield biomethane. Biogas pre-dominantly consists of CH_4 (40–75%vol) and CO_2 (16–60%vol), but depending on the utilized substrate and biological conversion process, traces of different other species can also be present (e.g., H_2S, NH_3, O_2, N_2, CO, HC's or siloxanes) [2]. Thus, the transformation of biogas to biomethane typically requires various gas-cleaning steps for removal of trace components as well as an upgrading step, in which CO_2 is removed to yield a biomethane stream with high calorific value. The required biomethane quality (e.g., for injection into the natural gas grid) is defined by national regulations and thus differs between the countries [1, 3]. However, depending on the country and application, biomethane contains 95–97% CH_4 and 1–3% CO_2 [2]. Due to the significant amount of CO_2 that needs to be removed from the raw biogas stream prior to grid injection, the economics of biogas upgrading are typically governed by the CO_2 separation step.

Today, there are various CO_2 separation processes deployed for biogas upgrading, with the main being amine scrubbing, pressure swing adsorption, physical absorption (water scrubbing, organic solvent scrubbing), and membrane

✉ Elisabeth Sonnleitner
elisabeth.sonnleitner@tuwien.ac.at

Gerhard Schöny
gerhard.schoeny@tuwien.ac.at

Hermann Hofbauer
hermann.hofbauer@tuwien.ac.at

[1] Institute of Chemical Engineering, Technische Universität Wien, Getreidemarkt 9, 1060 Vienna, Austria

separation [4–6]. While the individual processes obviously show some differences from a technological point of view, it was pointed out that the corresponding upgrading costs equalize with increasing upgrading capacity [7, 8]. Hence, it can be stated that currently, there is no single optimum biogas upgrading technology available. Instead, the final selection of a specific upgrading technology is mostly governed by local site conditions and by regional quality standards.

However, among the currently deployed technologies, amine scrubbing shows some outstanding advantages. In amine-scrubbing plants, the pre-treated biogas is passed through an absorber column where it is contacted with an aqueous amine solution (typically monoethanolamine (MEA), diethanolamine (DEA), or methyldiethanolamine (DMEA)). In the absorber, the CO_2 present in the biogas stream is absorbed by the solvent and reacts chemically with the dissolved amine components. The CO_2-rich solvent is continuously sent to the stripper where it is heated up (> 120–150 °C) to desorb the CO_2 again and to obtain a regenerated, CO_2-lean solvent that can be sent back to the absorber. Since the utilized solvents show a high affinity and selectivity towards CO_2, the biogas stream can be treated at low operating pressure. Thus, further compression of the biogas upstream to the absorber is typically not needed which gives a significant benefit, especially if the required pressure level of the application that utilizes the biomethane is low. Furthermore, in amine-scrubbing units, the CO_2 separation efficiencies and consequently the methane contents in the obtained biomethane are high while at the same time the methane slip to the stripper off-gas can be kept at a very low level [1, 2]. Consequently, the achievable methane recovery rates are high and the methane emissions of the process are low enough to avoid the need for further downstream gas treatment measures. The major disadvantage of this technology, however, results from the high heat input at relatively high temperature that is required for solvent regeneration in the stripper. Furthermore, due to the contact with the aqueous amine solution, the obtained biomethane stream is saturated with water and needs to be dried before it can be sent to compression. Another typical problem associated with this process is that the degradation products of the utilized solvents could lead to equipment corrosion and to harmful emissions of aerosols and nitrosamines. To improve the amine scrubbing process, current research is focusing on reducing the energy demand in the stripper through the development of new amine solvents and improved heat integration measures in the process. Research is also carried out on ways to utilize excess heat, for the regeneration of the solvent, with new systems proposed for biogas upgrading that can be regenerated at lower temperature compared to the conventionally used amine solvents [9, 10].

More recently, it has been proposed to utilize solid adsorbent materials instead of aqueous amine solutions. Similar to the amine-scrubbing process, the adsorbent materials can be utilized in a continuous temperature swing process for selective CO_2 separation. The major difference, however, is that the expected separation energy demand of the adsorption process could be significantly smaller. This is mainly due to the facts that no water evaporation occurs in the stripper column and that, compared to the conventionally used aqueous amine solutions, the adsorbent material also has a lower heat capacity. It has been further noted that in an adsorption process, the corrosion and emission issues are less critical and could be even almost eliminated if the right adsorbent materials are used [11]. Another benefit of the adsorption process is that the utilized adsorbents provide large specific surface areas that can facilitate prompt reactions between the active adsorption sites and the gas-phase CO_2. Consequently, the process equipment could be built smaller which could entail further reductions of the CO_2 separation costs by reducing the associated investment costs.

The basic set-up of a continuous temperature swing adsorption (TSA) process for biogas upgrading consists of an adsorber, operating at low temperatures, and a desorber, operating at higher temperatures. In the adsorber, the solid sorbent material selectively adsorbs the CO_2 present in the pre-treated biogas stream. Since adsorption is an exothermic process, the adsorber needs to be cooled in order to maintain the desired operating temperature of typically 40–70 °C. The CO_2-loaded adsorbent is continuously extracted from the adsorber and sent into the desorber. The desorber needs to be heated, in order to provide the sensible heat for the colder adsorbent stream, coming from the adsorber and to drive the endothermic desorption of CO_2. A stripping gas may be utilized in the desorber to further promote CO_2 desorption by keeping the CO_2 partial pressure low. This allows for deep regeneration of the adsorbent material, which is essential to achieve high CO_2 separation efficiencies. In post-combustion CO_2 capture applications, steam has been proposed as suitable stripping agent, since it can easily be separated from the desired CO_2 product by downstream condensation of the desorber off-gas. In biogas upgrading applications, air may be used as stripping agent instead, to save on operational costs for steam production. However, for some adsorbent materials, the presence of oxygen in combination with higher operating temperatures might lead to increased adsorbent degradation [12, 13]. Hence, depending on the utilized adsorbent material, the desorber inventory and operating temperature could be limited in case air is used as stripping agent.

The authors of this work most recently proposed and developed a novel reactor design for a continuous TSA CO_2 capture process [14, 15]. The system applies multi-stage fluidized bed columns in the adsorber and desorber that allow for effective heat integration and efficient process operation, through establishment of counter-current contact of gas and sorbent streams (Fig. 1). The feasibility of the system for post-

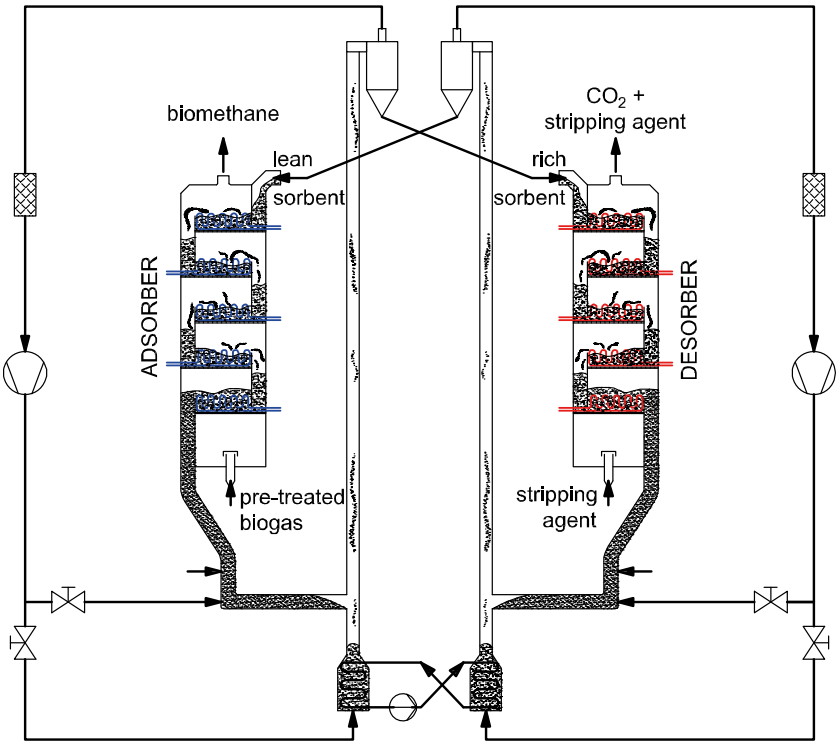

Fig. 1 Multistage fluidized bed reactor system for continuous TSA CO_2 capture

combustion CO_2 capture applications was recently demonstrated in experiments conducted within a fully integrated TSA bench scale unit [16]. The idea is to apply the same reactor system for biogas upgrading applications. However, due to the different separation tasks in post-combustion CO_2 capture and biogas upgrading applications (i.e., larger amount of CO_2 that needs to be removed, higher CO_2 partial pressures), the adsorber design will most likely be needed to adapt and potentially also, each of the processes will have its own optimal adsorbent material.

In the past, there have been many solid sorbent materials tested and proposed for CO_2 capture, in either post- or pre-combustion capture applications [17]. So far, several solid adsorbent materials have been in use already for pressure swing adsorption processes, where high adsorption capacities under elevated pressure are required [18, 19]. Among the most commonly applied adsorbent types are activated carbons and zeolites [17, 18, 20–25]. Activated carbons are well-studied adsorbent materials for CO_2 capture and are commonly applied because of their low price and easy availability. However, due to their relatively low CO_2 capacity at ambient pressure and at temperatures above 40 °C, they may not be suitable for application in the considered TSA process [17, 24–26]. On the contrary, zeolite-type adsorbents, also known as molecular sieves, typically show a very high CO_2 capacity and a high selectivity at the mentioned operating conditions. They are porous crystalline aluminosilicates, where the aluminum atoms introduce negative framework charges, which are compensated with exchangeable cations in the pore space [17]. As the type of the cation influences the strength of the electric field inside the pores, as well as the available pore volume, the cation is the essential factor that determines whether a zeolite is suitable for adsorption of a certain molecule or not [27]. In total, there are more than 230 different types of zeolites known by now, which differ in their SiO_2/Al_2O_3 ratio and the type and amount of applied cations [28]. Li et al. [22] tested and evaluated six different adsorbents for the separation of CO_2 and CH_4. Out of these six different zeolites, NaX and CaA were identified as the most promising adsorbents due to their high capacity for CO_2 uptake and their good CO_2/CH_4 selectivity of 76 (NaX) and 74(CaA). In another study conducted by Montanari et al. [23], the adsorption capacity of CO_2 and CH_4 on NaX was also tested and they rated the CH_4 adsorption as negligible.

More recently, solid amine sorbents have been proposed and developed as new adsorbent class for post-combustion CO_2 capture applications [13, 29–31]. In general, these materials consist of a porous polymeric, organic, or inorganic support, on which functional amine groups are immobilized. The amine can be either physically adsorbed (e.g., by wet impregnation), or covalently bound to the support's surface [17]. However, for the application in a TSA process, the thermal stability of the material is of special importance. Therefore, the latter adsorbent type with amine groups covalently bond to the support may be preferred, as they showed to be more stable [17, 32]. Similar as within liquid amine systems, bulk gas CO_2 can be selectively separated through chemical reaction with the active amine sites. Thus, it can be expected that the

achievable methane purities and recovery rates in a TSA biogas upgrading process that utilizes amine-functionalized adsorbent materials are similarly high as for amine-scrubbing processes. Nevertheless, as most of the solid amine sorbents are proposed for post-combustion capture, there is hardly any rating in the literature regarding CH_4 adsorption on these materials.

In this work, a zeolite and a solid amine-type sorbent are evaluated for application in the proposed TSA system. The first part of the material evaluation included measurements of CO_2 and CH_4 adsorption isotherms, for assessment of the adsorption selectivity as well as an evaluation of the mechanical and thermal stability of both adsorbent materials. In the second part of the material evaluation, the experimentally derived adsorption data was used to establish mathematical adsorption models for both materials. The adsorption models were then introduced into an existing process simulation tool that has previously been used for a thermodynamic evaluation of the TSA process for CO_2 capture from flue gas streams [14]. Finally, process simulations were performed to assess the expectable regeneration energy demand of the TSA biogas upgrading process for both the tested materials and the different operating conditions.

2 Methods

2.1 Materials

Based on the mentioned findings, reported by Li [22] and Montanari [23] for NaX-type adsorbents (also known as Zeolite 13X), this material was identified as potential adsorbent material for the proposed TSA process. However, it was decided to perform an own experimental evaluation on a 13X zeolite. This is because previous studies provide contradictory information about the CH_4 adsorption capacity of zeolite 13X [20, 22, 23] and since information about the applicability of this adsorbent material in fluidized bed systems is lacking. The specific material used in the experiments is the commercially available adsorbent material 13X MOLSIV™ provided by Honeywell UOP (hereafter called "13X"). The most important material data, extracted from the material datasheet, is given in Table 1.

From the group of solid amine sorbents, the ion-exchange material Lewatit® VP OC 1065 (hereafter called "Lewatit"), from the manufacturer Lanxess, was chosen as second potential adsorbent for the proposed TSA process. The material consists of a polystyrene polymer, which is cross-linked with divinylbenzene and functionalized with primary amine groups, through a phthalimide process [33]. This adsorbent was proposed for example by Veneman et al. [34] for application in continuous TSA CO_2 capture processes. In several studies, this material was considered as thermally and mechanically stable and showed excellent CO_2 capture properties [29, 34, 35]. These previous studies assessed the adsorption behavior of CO_2 and H_2O on Lewatit for the purpose of carbon capture from flue gas. However, so far, Lewatit has not been considered for utilization in biogas upgrading applications, except by Sutanto et al. in their recently published study [36]. Hence, only little information on CO_2/CH_4 separation properties of Lewatit are available. This fact triggered the adsorption tests performed with Lewatit in this work.

Table 1 Material properties of the tested adsorbents

	Lewatit	13X
Composition	Cross-linked polystyrene functionalized with primary amines	Clay bound NaX
Average particle diameter	0.52 mm	1.4 mm
Average pore diameter	25 nm	0.8 nm
Bulk density	630–710 kg m^{-3}	641 kg m^{-3}

2.2 Experimental set-ups

2.2.1 Fixed bed reactor tests

The fixed bed set-up consisted of three mass flow controllers (MFCs), a fixed bed reactor (reactor inner diameter 50 mm, solids bed height 55 mm measured from gas feeding location) with jacket heating and internal heating bars, and a non-dispersive-infrared (NDIR) gas analysis of the gas at the outlet of the reactor. The scheme of the set-up is displayed in Fig. 2. Prior to the experiments, the materials were dried in the fixed bed. For this purpose, the reactor was heated up to 100 °C and purged for 4 h with N_2. After the 4 h of drying, the material was considered as dry and extracted from the reactor, followed

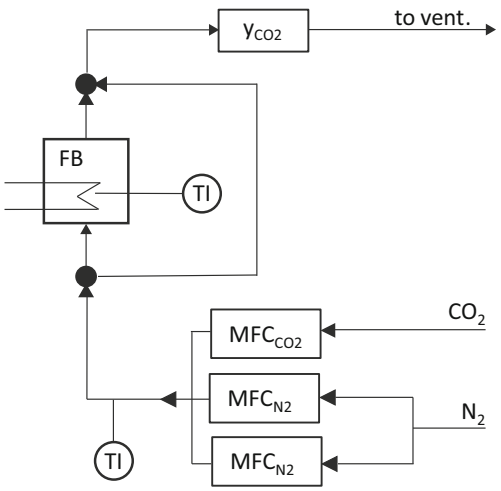

Fig. 2 Scheme of fixed bed set-up

by instant weighting on an analytical balance to receive individual samples of 10–30 g. For the measurements of the adsorption isotherms, the reactor was filled partially with silica sand, which is considered as inert regarding adsorption of either N_2, CO_2, or CH_4. The derived samples were placed on top of the silica sand in order to ensure a proper placement in the reactor (i.e., in the location of the heating bars), as displayed in Fig. 3. As initial step for each trial, the reactor was heated to 100 °C and purged with N_2, until no more CO_2 could be detected in the off gas. Afterwards, the reactor was cooled down to the desired adsorption temperature. As soon as the temperature was stable, the first CO_2 concentration was set. For this, the total gas volume flow of 50 l/h was split to the desired CO_2 volume flow, which was balanced with N_2. The CO_2 concentration was kept until the equilibrium loading was reached and the signal, measured at the gas analysis, was stable over about 10 min. Subsequently, the CO_2 concentration was increased stepwise to determine five to seven equilibrium loadings at CO_2 partial pressures between 0.02 and 0.5 bar. At the end of each isothermal measurement, the sample was regenerated at 100 °C with N_2.

To obtain the respective isotherm, the difference between measured gas concentration in the off gas and the end concentration after breakthrough was determined for each recording interval of 5 s. With the total gas volume stream set at the MFCs and the concentration change, the adsorbed volume could be calculated. The adsorbed mass of CO_2 was related to the total dry sample weight. For each measured CO_2 concentration profile, a reference measurement was carried out with only inert material in the reactor. With the reference measurement, the inert response of the system was determined. The received response of the inert system was afterwards subtracted from the results obtained with the adsorbent sample, in order to account for delay times in the experimental setup and thus to avoid an over-estimation of the adsorbed gas (Fig. 4). The used gases were N_2 and CO_2, both grade 5.0.

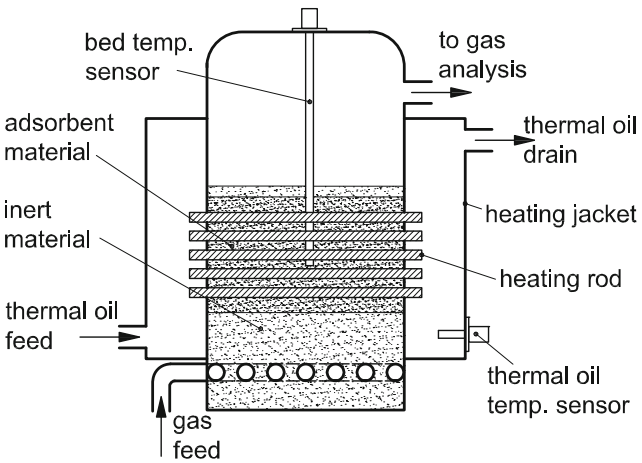

Fig. 3 Fixed bed reactor

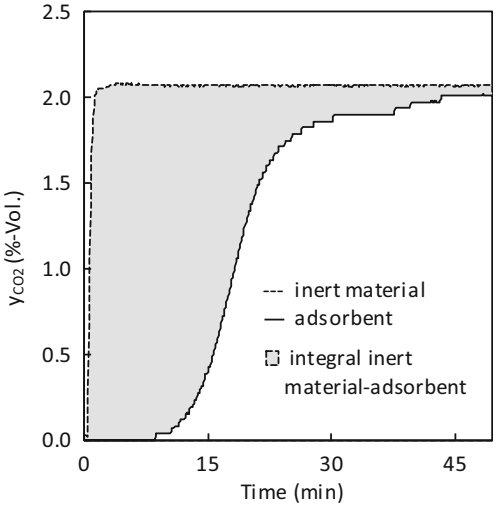

Fig. 4 CO_2 breakthrough curve from 0 to 2% CO_2, once with adsorbent material and once the reference measurement with inert material, at 60 °C

2.2.2 TGA measurements

For the TGA measurements, a NETZSCH STA 409 PC Luxx® was used. The TGA has two different gas inlets, one for the protective gas stream over the balance and a second one for the reactive gas stream, which both are mixed at the entry to the sample chamber. For the protective gas stream, only inert gas, such as N_2, may be used and the volume stream must be greater than the reactive gas stream. The reactive gas stream used in the experiments contained either CO_2, CH_4, or any mixture thereof, as well as a N_2/O_2 mixture for the regeneration and thermal stability tests. In the present measurements, a total gas stream of 100 ml min^{-1} was chosen, whereof a constant protective stream of 55 ml min^{-1} N_2 was used. The flows of the individual gas species were controlled via five MFCs. Prior to each adsorption test, a conditioning step was performed to desorb any preadsorbed CO_2 and moisture. Therefore, the sample was heated to 95 °C under a N_2 stream and kept at these conditions for about 1.5 h. This time span was enough to reach a constant mass signal at the end of the conditioning step. Afterwards, the sample was cooled to the desired adsorption temperature. As soon as the signal was stable, the composition of the reactive gas stream was adjusted and the adsorption test started. For all tests performed with CO_2, a mass increase of the adsorbent sample was detectable immediately after CO_2 was introduced into the sample chamber. It was assumed that the adsorbent sample reached its equilibrium adsorption capacity for the prevailing test conditions when there was no further mass change detectable. After adsorption equilibrium was reached, either another adsorption step at a higher concentration of the adsorptive or a desorption step for complete regeneration of the adsorbent sample followed. For the CO_2 and CH_4 isotherms, the reactive gas concentration was increased stepwise, from 2 to 45%. The reactive gas stream consisted of the desired CO_2 or CH_4 concentration, which was balanced with N_2 to a total stream of 45 ml min^{-1}. The

measurements with mixed gases of CO_2 and CH_4 were performed with a CO_2 gas stream of 4 ml min^{-1} and a CH_4 stream of 41 ml min^{-1}. To simulate air, an O_2 stream of 20 ml min^{-1} was mixed with a total of 80 ml min^{-1} N_2.

Each measurement was performed twice: once with the sample and a second time without the sample. Afterwards, the gravimetric signal of the empty measurement was subtracted from the measurement with sample, to correct for influences of changing operating temperatures and gas compositions on the buoyancy of the sample probe. The corrected mass change per adsorption step was then related to the dry sample mass (i.e., the sample mass after the conditioning step) to obtain the specific equilibrium loading of the adsorbent material. The used gases, within the TGA measurements, were CO_2 grade 4.8, CH_4 grade 4.5, N_2 grade 5.0, and O_2 grade 5.0.

2.2.3 Fluidization tests

The fluidization test rig for evaluation of the mechanical stability of the adsorbent materials consisted of an acrylic glass tube (inner diameter = 50 mm) and a perforated plate-type gas distributor (Fig. 5). Compressed air was used as fluidization gas and supplied into the plenum beneath the gas distributor. After the adsorbent materials were placed on the gas distributor, a filter was mounted to the top of the glass tube. The lamellar tissue filter is sufficient to collect the small particle fractions that may be formed during the fluidization tests due to abrasion and fragmentation of the adsorbent material. In regular intervals, the weight of the set-up containing the remaining sample as well as the filter was weighted on a balance. The weight loss of the material in the test rig was crosschecked with the weight of particles collected in the filter, to avoid any interference of varying room temperatures and humidities during the test. Prior to the fluidization tests, the material was conditioned by purging with compressed air for 48 h. For this conditioning step, the air stream was kept below minimum fluidization velocity to avoid attrition. The conditioning step was necessary, to prevent any interference of the measured weight loss, due to drying, moistening, or adsorption of components in the compressed air.

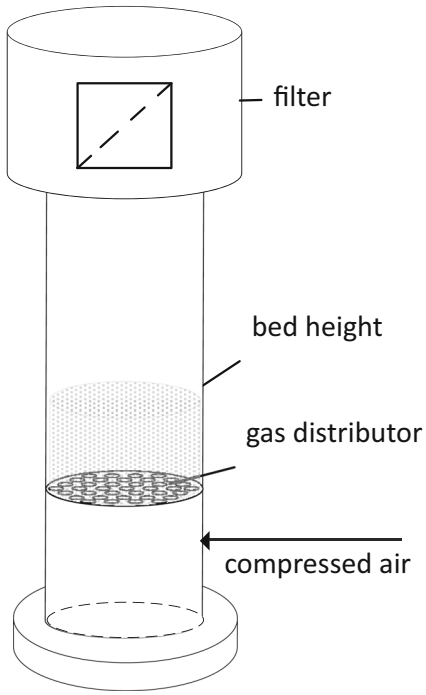

Fig. 5 Scheme of fluidization test rig

The minimum fluidization velocity U_{mf} was determined experimentally in the same test rig, by a stepwise decrease of the superficial gas velocity from above to below fluidization conditions (i.e., from a fluidized bed to a fixed bed) while measuring the resulting pressure drop over the test rig. First, this procedure was conducted without material to determine the pressure drop of the gas distributor that needs to be subtracted from the measured pressure drops obtained with a bed material. The minimum fluidization velocity was then determined by intersecting the obtained linear correlation, between the superficial gas velocity and the bed pressure drop over the fixed bed, with the constant pressure drop obtained for the fluidized bed of adsorbent material.

2.3 Modeling

2.3.1 Adsorption equilibrium modeling

The adsorption models by Langmuir and Toth were used in this work to derive suitable mathematical descriptions of the experimentally determined CO_2 adsorption equilibria data of both adsorbent materials [37]. The Langmuir model assumes a monolayer adsorption (Eqs. (1 and 2)) on the adsorbent material. The temperature-dependent Toth model is a semi-empirical model, which also accounts for sub-monolayer coverage (Eqs. (3–7)). In the Langmuir model, the maximum adsorption capacity q_{max} corresponds to a complete monolayer coverage of the adsorbent and is thus temperature independent. The parameter ΔH_{ADS} reflects the heat of adsorption, which is considered to be equal for each adsorption site and the parameter b, the so-called Langmuir constant, reflects the affinity of the attraction of an adsorbate to the surface.

Langmuir model (adapted from [37]):

$$\theta = \frac{q}{q_{max}} = \frac{b\, p_{CO_2}}{1 + b\, p_{CO_2}} \quad (1)$$

$$b = b_\infty \exp\left[-\frac{\Delta H_{ADS}}{R\, T}\right] \quad (2)$$

In the Toth model, the maximum loading n_s is temperature dependent and compared to the Langmuir model, an additional parameter t is added. The parameter t is a characterization for the systems heterogeneity. The suffix 0 for the parameters

t_0 and b_0 indicates that they have to be found at a reference temperature T_0, whereby in this work, T_0 was selected with 343 K. ΔH again represents the heat of adsorption, whereas ΔH_0 reflects the heat of adsorption at zero coverage. The parameters α and χ are constant parameters to describe the temperature dependency of the corresponding model parameters t and n_s.

Toth model (adapted from [37]):

$$q = \left[\frac{n_S b\, p_{CO_2}}{\left(1 + \left(b\, p_{CO_2}\right)^t\right)^{\frac{1}{t}}}\right] \tag{3}$$

$$b = b_0 \exp\left[\frac{\Delta H_0}{R\, T_0}\left(\frac{T_0}{T} - 1\right)\right] \tag{4}$$

$$n_S = n_{S0} \exp\left[\chi\left(1 - \frac{T}{T_0}\right)\right] \tag{5}$$

$$t = t_0 + \alpha\left(1 - \frac{T_0}{T}\right) \tag{6}$$

$$-\Delta H = \Delta H_0 - \frac{1}{t}(\alpha R T_0)\left\{\ln(b\, p) - \left[1 + (b\, p)^t\right]\ln\left[\frac{b\, p}{\left(1 + (b\, p)^t\right)^{1/t}}\right]\right\} \tag{7}$$

2.3.2 TSA process modeling

Simulations of the multistage fluidized bed TSA process were performed with an existing IPSE Pro5.1 simulation tool. The process model is based on the model that was previously introduced by Pröll et al. [14]. The core of the simulation tool is represented by individual fluidized bed stage unit models that are connected to reassemble a 5 × 5 stage TSA process set-up (see Fig. 6). Isothermal operating conditions as well as ideal gas-solids contact and ideal mixing of the fluidized sorbent material are assumed for each stage unit. Furthermore, adsorption equilibrium is considered to be reached and the corresponding equilibrium sorbent loadings are calculated by using one of the adsorption models described above. The assumption of having ideally mixed solids requires the CO_2 partial pressure in the outgoing gas stream to be determined by the equilibrium loading of the sorbent material within the stage. Heat exchangers are included for supply of the required cooling and heating demand in each stage. For the sake of simplicity, the adsorbent materials are considered to exclusively interact with CO_2 that is present within the gas streams. This means, it is not possible to study the impact of co-adsorption of other gas species like CH_4 or H_2O in this rather simple model. However, differences in the gas compositions are considered in the energy balances by accounting for the corresponding heat capacities of the individual gas streams. Furthermore, a lean-rich-heat recovery, as proposed by Pröll et al. [14], or other potential heat integration measures were not considered in the model.

The gas feeding rates chosen for the simulations were 12 $Nm^3\ h^{-1}$ and 7 $Nm^3\ h^{-1}$ for the adsorber and desorber, respectively, based on typical operation conditions in a bench-scale unit [16]. The CO_2 content of the raw biogas was assumed to be 40% in accordance with the average composition of biogas derived from anaerobic digestion of agricultural waste [1, 2, 5]. Ambient air at 20 °C is used as stripping agent in the desorber column, whereas a blower was incorporated in the model to provide the required pressure elevation of that stream. The blower power is, however, not added to the process regeneration energy demand. The specific thermal regeneration energy requirements of the TSA process that are reported in this work were determined by summation of the heating demands in the individual desorber stages and by relating this heating demand to the product gas stream leaving the adsorber column. As pointed out above, the heating demand in the individual desorber stages arise from the latent heat demand for desorption of CO_2 and the sensible heating demand for lifting the temperature of the incoming sorbent and stripping gas streams to the desorber operating temperature.

In the process simulations performed in this work, the adsorber stages were considered to be operating at a constant temperature of 50 °C. The desorber stages were also considered to be operated at the same temperature, but in contrast to the adsorber, the desorber temperature was varied in a

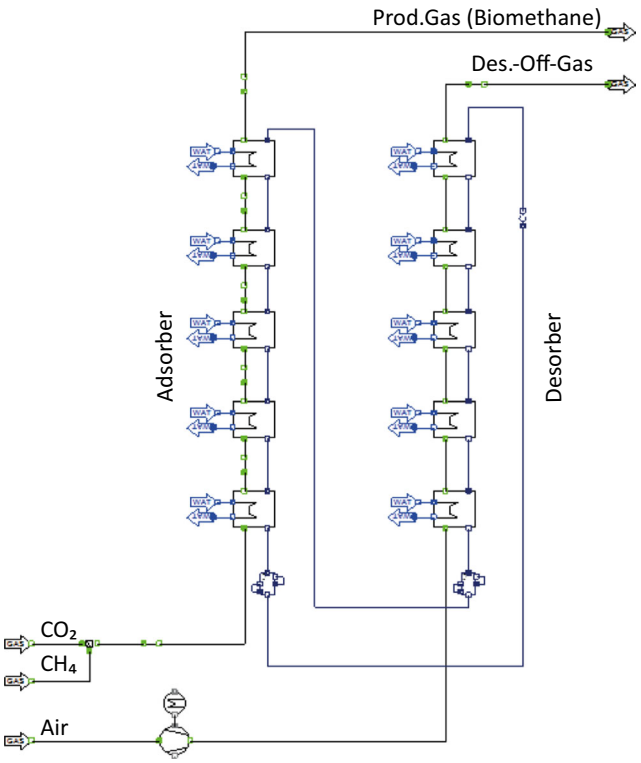

Fig. 6 TSA process simulation model in IPSE Pro5.1

temperature range of 80–120 °C to assess the impact of varying temperature swings on the derived regeneration energy demand. Simultaneously, to the variation of the desorber temperature, a variation of the residual CO_2 content in the adsorber off-gas (i.e., the biomethane quality) has been performed. Due to different legislations that are in place among European countries, the biomethane standards can differ significantly with respect to the residual CO_2 content in the upgraded biomethane stream. For instance, the lowest limit of the residual CO_2 content for gas grid injection varies from ≤ 2%vol for gas grids in Austria [5] to up to 10.3%vol in the Netherlands [1]. In accordance to these values, the residual CO_2 content in the off-gas stream of the adsorber column has been varied from 2 to 10%vol.

3 Results and discussion

3.1 Experimental results

3.1.1 CO_2 capacity

Adsorption experiments were carried out using the fixed bed reactor as well as the TGA. The CO_2 capacity measurements were performed by gradually increasing the partial pressure of CO_2 while maintaining isothermal conditions. For each partial pressure, an equilibrium loading was reached. These equilibrium loadings are represented by the data points for the respective isotherms, displayed in Figs. 7 and 8. The isothermal measurements were performed at 40, 60, and 95 °C/102 °C. The highest measured capacities at 40 °C were 2.5 mol kg^{-1} for Lewatit and 3.6 mol kg^{-1} for 13X, at the highest investigated CO_2 partial pressure of 0.5 bar. Both materials show a high CO_2 capacity but different uptake behavior. While 13X

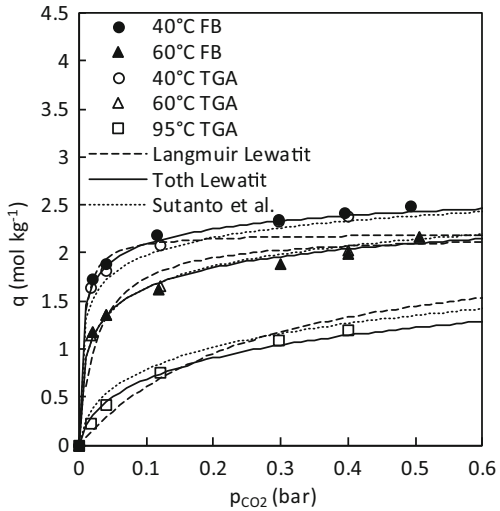

Fig. 7 CO_2 adsorption isotherms on Lewatit obtained from FB and TGA measurements with fitted Langmuir and Toth model, Toth model by Sutanto et al. [36] for comparison

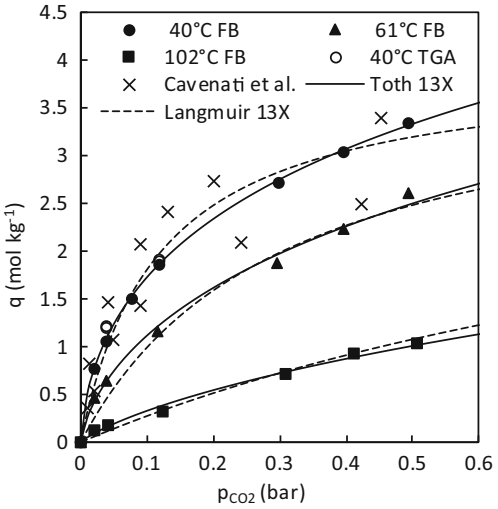

Fig. 8 CO_2 adsorption isotherms on 13X obtained from FB and TGA measurements with fitted Langmuir and Toth model, CO_2 adsorption isotherms by Cavenati et al. [20] at 35 and 50 °C for comparison

provides higher capacity at CO_2 contents above about 12%, Lewatit performs better at CO_2 contents below about 12%. A high CO_2 equilibrium loading of the adsorbent material at low CO_2 partial pressures is obviously an advantage for reaching the required low CO_2 concentrations in the biomethane (< 3%). On the other hand, for lower biomethane purity standards, the higher capacity of 13X would be beneficial in order to decrease the required solid circulation rate in the system. The CO_2 adsorption enthalpy of both materials was calculated by using the Clausius-Clapeyron equation. The calculated adsorption enthalpies are 43 kJ mol^{-1} for 13X and 76 kJ mol^{-1} for Lewatit. These enthalpies have been calculated for a reference temperature of 50 °C and loading of 1.8 mol kg^{-1} (Lewatit) and 0.82 mol kg^{-1} (13X), and they are very well in line with the values reported by Li et al. [22] and Veneman et al. [35]. The obtained adsorption enthalpies are also well in line with the expected adsorption mechanisms (i.e., physisorption for 13X vs. chemisorption for Lewatit) for both materials.

For the measurements in the TGA, the pre-dried Lewatit, which was prepared for the fixed bed measurements, was used. During the first conditioning step, an additional weight loss of 16.8% was measured, which led to the conclusion that the drying was not complete. Therefore, the pure CO_2 adsorption isotherms were repeated in TGA. It is expected that the material dried in the pre-conditioning step in the FB is the same as that detected in the TGA. As the loading is referred to the dry sample mass, which was weighted after the 4 h of drying in the FB, it was decided to correct the data points obtained from the FB measurements. This correction was performed by reducing the dry sample weight, on which the adsorbed CO_2 mass was balanced, by 16.8%. In Fig. 7, the corrected FB values are displayed. For future measurements, FB is considered as a reliable source for adsorption

measurements, as long as the drying step is extended according to the moisture content of the sample. For 13X, no additional mass loss was measured in the TGA, which matches the indication in the material delivery datasheet, provided by the supplier, that 13X is dry. As the isotherms for 13X fit very well to literature references [20, 38] and no additional drying occurred, it was not repeated in TGA but taken from the FB results.

The received CO_2 isotherms for Lewatit match the capacities reported by Yu et al. [12], who reported 2.15 mol kg^{-1} (40 °C, p_{CO2} 0,15 bar) and Sutanto et al. [36] (Toth model by Sutanto et al. displayed in Fig. 7) but are below the capacities reported by Veneman et al. [35]. At 60 °C, the model presented by Sutanto et al. shows an exact overlap with the measured equilibrium loadings. However, the model predicts slightly larger equilibrium loadings at higher and lower equilibrium loadings at lower operating temperatures.

3.1.2 Selectivity

In order to determine the selectivity of Lewatit and 13X towards CO_2 adsorption, several tests have been performed with pure CH_4 and different mixtures of CH_4 and CO_2. Furthermore, adsorption tests have been carried out with alternating flows of CH_4 and CO_2. At first, the adsorption isotherms for pure CH_4 were measured analog to the CO_2 isotherms in the TGA for both materials. The CH_4 adsorption capacities were measured at 40 and 60 °C and for concentrations of 5–45% CH_4. For Lewatit, no significant CH_4 adsorption was detectable on the mass signal of the TGA and even a small overall mass loss of the adsorbent sample was encountered at increasing CH_4 contents during measurement of the 40 °C isotherm (Fig. 9). The empty reference measurement, which was conducted to correct the effects of buoyancy and the drift of the scale, showed mass changes in the same order as the measurement with Lewatit. Hence, it was concluded that no significant CH_4 adsorption occurs on Lewatit or that CH_4 adsorption on Lewatit is at least not detectable with the applied method. This is also in line with CH_4 adsorption studies with other amine-functionalized materials [39] and with findings from Sutanto et al. for Lewatit [36].

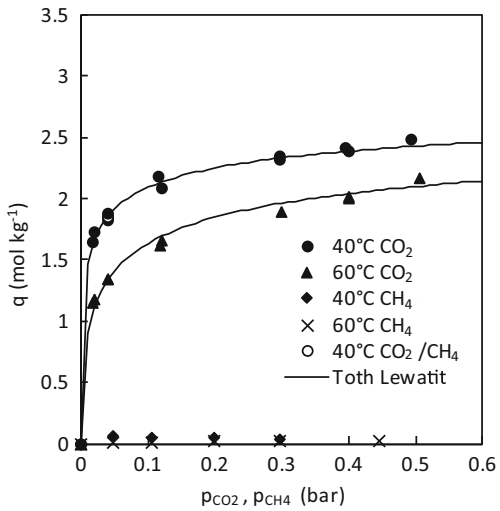

Fig. 9 CH_4 adsorption on Lewatit in comparison to CO_2 adsorption

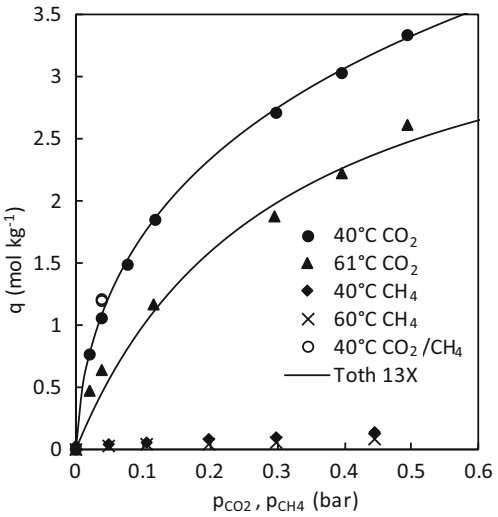

Fig. 10 CH_4 adsorption on 13X in comparison to CO_2 adsorption

For 13X, a constant, slight mass increase was detectable when the sorbent sample was exposed to the N_2/CH_4 gas mixture. The maximum measured mass gain of the 13X sample corresponded to 0.2 wt% (0.13 mol kg^{-1}) at 40 °C and 0.45 bar partial pressure. However, in all TGA measurements with 13X, a slight constant mass increase even during conditioning phase was detected. As there was no gas analysis available, to measure the adsorbed species in TGA, the origin of the adsorbed mass cannot be fully clarified. Cavenati et al. [20] reported an adsorption of N_2 on 13X, which is approximately in the same quantity as CH_4 adsorption. Therefore, it might be that part of the detected mass change could be attributed to N_2 adsorption. However, since the measured mass changes are comparably small, it was assumed that CH_4 adsorption on 13X can be neglected for further process evaluation in this work (Fig. 10). This assumption is also supported by work performed by Montanari et al. in which no CH_4 adsorption was measured on 13X [23]. Nevertheless, it is worth to mention that other authors, such as Cavenati et al., Li et al., and Mulgundmath et al. [20, 22, 40], reported that small amounts of CH_4 are adsorbed by 13X. Compared to the measured relative mass changes in this work, the reported values are approximately twice as high. Cavenati et al. measured 0.2 mol kg^{-1} at 35 °C, whereas Li et al. measured 0.35 mol kg^{-1} at 30 °C and Mulgundmath et al. measured 0.24 mol kg^{-1} at 40 °C, all at a CH_4 partial pressure of 0.4 bar.

In order to investigate if the presence of CH_4 influences the CO_2 adsorption behavior of the adsorbent materials, two

Table 2 CO_2/CH_4 mixed gas adsorption compared to pure CO_2 adsorption capacity at 40 °C

	p_{CO2} (bar)	p_{CH4} (bar)	p_{N2} (bar)	Lewatit CO_2 loading (wt%)	13X CO_2 loading (wt%)
First adsorption	0.04	0.41	0.55	8.16%	5.23%
Second adsorption	0.04	0.41	0.55	8.17%	5.30%
Reference	0.04	0.00	0.96	8.00% (TGA)	4.65% (FB)

subsequent adsorption measurements have been performed with CO_2/CH_4 mixtures. The measured CO_2 loadings were then compared to the reference values obtained from pure CO_2 adsorption tests. For Lewatit, no influence of CH_4 could be detected and the measured CO_2 loading was in line with the reference value as displayed in Table 2. The adsorbed mass on 13X was higher than the reference point obtained in the FB measurement. Since the additional mass uptake could not come from CH_4 adsorption, it was concluded that adsorption equilibrium was not reached in the reference point from FB measurements at 4% CO_2 (see Fig. 8).

In addition to the adsorption tests with CH_4/CO_2 mixtures, further tests with alternating gas flows of CO_2 and CH_4 were performed. Figure 11 shows the results obtained from the measurement where a sample of Lewatit was first exposed to CO_2, followed by an exposure to a CO_2/CH_4 gas mixture and finally to pure CH_4. As expected, the addition of CH_4 did not cause any mass increase and in the second phase of pure CH_4, the sample mass even decreased, which indicates that the previously adsorbed CO_2 desorbed from the sample. In the second measurement, displayed in Fig. 12, the order of the used reactive gas mixtures was changed to first CH_4 exposure, followed by the CO_2/CH_4 gas mixture and finally to pure CO_2 exposure. For this measurement, the mass of the Lewatit sample was, however, three times larger as compared to the first one. The larger sample mass was selected for this measurement to be able to even detect small changes of the sample mass during CH_4 exposure. However, no mass change was detected during the CH_4 exposure period, which again indicated that no significant CH_4 adsorption occurs on Lewatit. Consequently, the adsorbent material should allow for very selective CO_2 removal from biogas with practically no methane slip arising from co-adsorption of CH_4. The higher sample mass caused, which in the selected time period for pure CO_2 exposure, the CO_2 equilibrium loading could not be reached.

3.1.3 Thermal degradation

TGA tests were performed to evaluate the thermal stability (e.g., loss of adsorption capacity) of both adsorbent materials, in order to assess potential limits of the desorber operating temperature. For this, the adsorbent samples were heated up from ambient temperature to 190 °C at a heating rate of 1 °C min^{-1} and the sample mass loss was recorded and considered as indication for degradation effects. Two experiments were conducted with both adsorbent materials. In the first experiment, the samples were exposed to nitrogen, whereas in the second experiment, the TGA chamber was continuously purged with simulated air to assess whether the presence of oxygen leads to an increased degradation of the

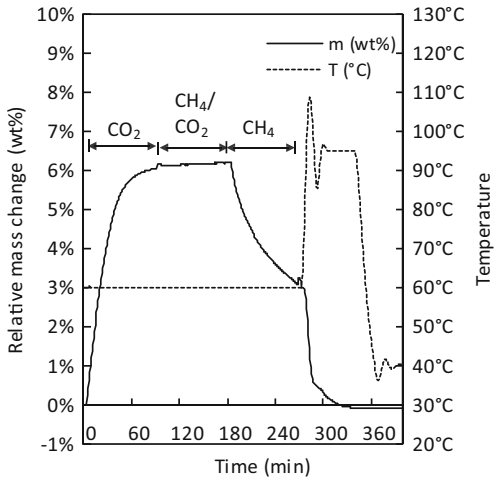

Fig. 11 Alternating adsorption of CO_2 (0.04 bar) → CH_4/CO_2 (0.41/0.04 bar) → CO_2 (0.04 bar) on Lewatit

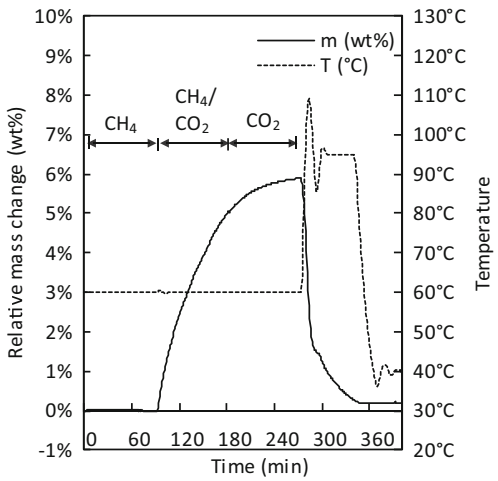

Fig. 12 Alternating adsorption of CH_4 (0.41 bar) → CH_4/CO_2 (0.41/0.04 bar) → CO_2 (0.04 bar) on Lewatit

adsorbent sample. The respective mass loss was measured and referred to the dry sample mass, as displayed in Figs. 13 and 14. In the first experiment with N_2 purge, Lewatit did not show any significant mass loss up to 110 °C. When purged with air, however, a slight mass loss was detected already at 90 °C and became more significant at 110 °C. While at 160 °C no further mass loss was detected with N_2, the presence of oxygen caused a further decrease. After the experiment, the Lewatit samples had changed their color from fawn to brown and the size of the individual particles was significantly smaller. In the material datasheet of Lewatit, a thermal stability up to 100 °C is claimed, which is even below the measured 110 °C. During the conducted measurements, only the mass loss was measured over a linear temperature increase. In contrast to the measured stability in the present experiments, a new study by Yu et al. [12] showed that the long-term stability of Lewatit in N_2 is given up to 150 °C. When exposed to air over several hours and days, Yu et al. measured a degradation already at 80 °C, leading to a 30% loss of the CO_2 adsorption capacity. Hallenbeck and Kitchin [41] performed experiments with adsorption at 50 °C and desorption at 120 °C in the presence of small oxygen concentrations of 4%vol. They concluded that the oxygen had no influence on the CO_2 adsorption capacity of the material over 17 cycles. On the other hand, they also performed adsorption tests with a Lewatit sample that was pre-treated in air at 120 °C, over 7 days. For this sample, a CO_2 adsorption capacity loss of 79% could be detected. In the elemental analysis, the loss of capacity could be attributed to a loss of adsorbent's nitrogen content [12, 41]. Nevertheless, in order to get more details on the effects of thermal degradation on the adsorption behavior of Lewatit, additional analysis would be needed. However, the obtained results indicate that with Lewatit, the desorber operating temperature has to be limited to around 100 °C in case air is used as stripping agent. Furthermore, the desorber inventory might need to be limited in order to keep the residence times in the hot environment low and to minimize adsorbent degradation effects.

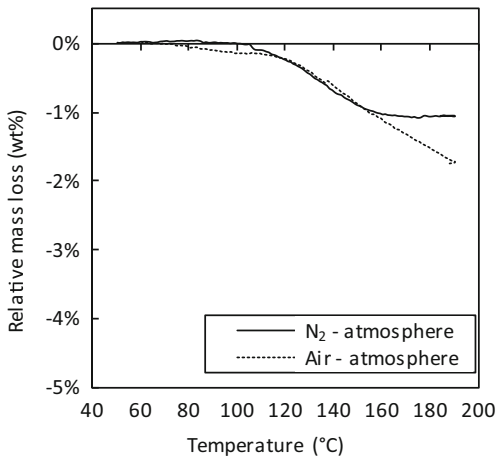

Fig. 13 Thermal stability of Lewatit

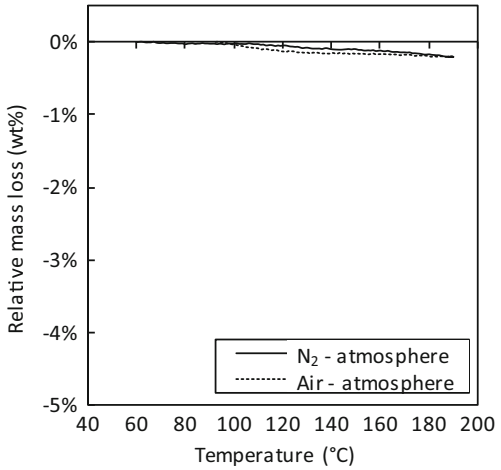

Fig. 14 Thermal stability of 13X

In contrast to the findings for Lewatit, 13X did not show a significant degradation (i.e., mass loss) up to 190 °C, regardless of the gas atmosphere (i.e., N_2 or air). This is also in line with the information provided in the material datasheet of 13X. Hence, it was concluded that the desorber operating temperature in the TSA process would not be limited by the thermal stability of 13X.

3.1.4 Regenerability

Next to adsorbent degradation, the desorber operating temperature may also influence the CO_2 desorption rates and consequently adsorbent regeneration in general. Preferably, the adsorbent material shows a sufficient regeneration rate at moderate desorber operating temperatures. Therefore, measurements with two adsorption cycles (at 40 °C with a CO_2 partial pressure of 0.12 bar), each followed by a desorption step with air, were performed. Based on the results obtained from the thermal degradation tests, the desorption step was performed at 95 °C for 1 h.

Lewatit reached a complete regeneration of the sample in both desorption steps. Additionally, no influence of the presence of O_2 at desorption could be detected during the second adsorption cycle. In both adsorption cycles, similar adsorption capacities were reached as within the CO_2 isotherm measurements. The mass uptake and loss during desorption is presented in Fig. 15. As displayed in Fig. 16, for 13X, no complete regeneration was reached after the first desorption cycle with air. Nevertheless, in the second desorption step, the same degree of regeneration could be reached as within the first one. Furthermore, in the second adsorption cycle, the same loading as in the first adsorption cycle was reached. This suggests that

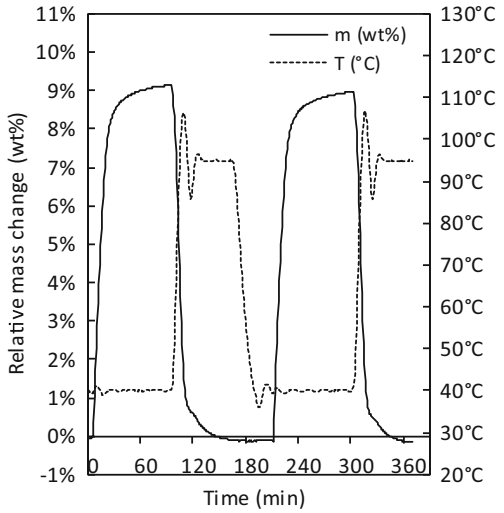

Fig. 15 Mass change of Lewatit during conditioning (95 °C), first adsorption (40 °C), desorption with air (95 °C), second adsorption (40 °C), and second desorption with air (95 °C)

the incomplete desorption results from the insufficient desorption time and/or temperature. The incomplete regeneration of 13X may lead to a reduced working capacity in a continuous process, in case the residence time or the operating temperature in the desorber cannot be selected sufficiently. Nevertheless, both Lewatit and 13X showed a high desorption rate at the beginning of the desorption step until around 90% of the regeneration was completed. Hence, it was concluded that the selected regeneration conditions should be sufficient for both adsorbent materials, considering the anyhow higher adsorption capacity of 13X and the proportionally low loss of working capacity.

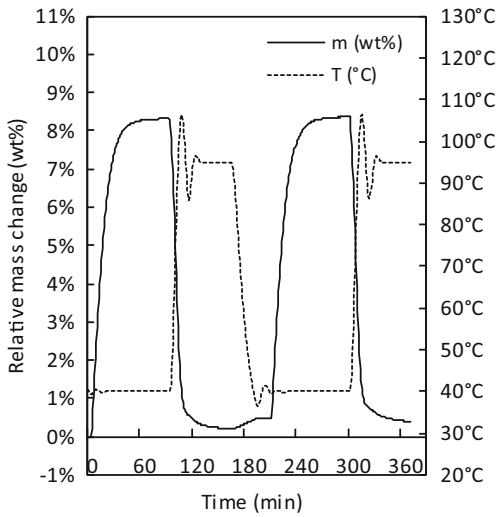

Fig. 16 Mass change of 13X during conditioning (95 °C), first adsorption (40 °C), desorption with air (95 °C), second adsorption (40 °C), and second desorption with air (95 °C)

3.1.5 Fluidization tests and mechanical stability

In order to evaluate the suitability of the selected adsorbent materials for application in the proposed fluidized bed reactor system, their fluidization properties and mechanical stability were assessed in the previously described fluidized bed test rig. At first, the minimum fluidization velocity at ambient conditions was determined for both materials. The measured minimum fluidization velocities were 0.47 m s^{-1} for 13X and 0.1 m s^{-1} for Lewatit, respectively. After determination of the minimum fluidization velocities, both materials were fluidized for more than 30 h with air at ambient temperature (20–25 °C) to assess their mechanical stability. During the experiment, the superficial gas velocity was set to 0.59 m s^{-1}, which resulted in a maximum gas velocity in the holes of the gas distributor in the range of 50 m s^{-1}. Apart from weight change, which was measured every few hours, also visual checks were done. Already after a runtime of only 5 h with the 13X batch, powdery dust was visible on the walls of the test rig and within the filter. In addition, the weight of the remaining bed of 13X decreased significantly with the further run time so that after 32 h, a relative weight loss of 4% was determined. On the contrary, Lewatit did not show any attrition or weight loss, even after 46 h of fluidization. The slight fluctuation, which can be seen in Fig. 17, most likely results from variations in the relative humidity of the fluidization air and to the accuracy of the balance. While the selected test procedure for assessment was rather simple, it clearly indicated that 13X is not suitable for application in a continuous fluidized bed process. Potentially other production forms of the zeolite (i.e., alternative binders) are required to improve its mechanical stability. In a real TSA process, the adsorbent material will be exposed to larger operating temperatures and gas velocities. Consequently, it is not possible to predict the mechanical stability of Lewatit under practical operating conditions

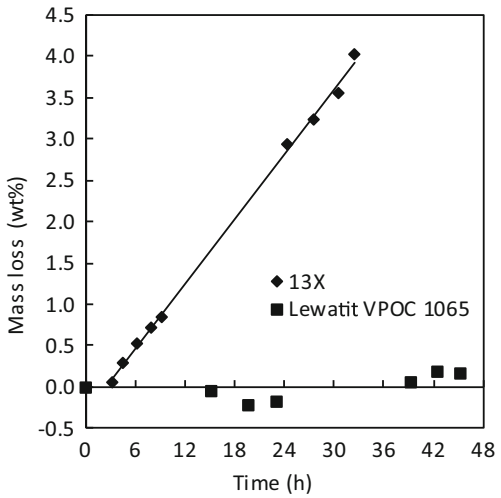

Fig. 17 Attrition of 13X and Lewatit in a fluidized bed

Table 3 Langmuir isotherm parameters

Langmuir parameters	Lewatit	13X
q_{max} (mol kg^{-1})	2.21	3.96
b_∞ (bar^{-1})	1.17×10^{-9}	3.23×10^{-6}
ΔH_{ADS} (kJ mol^{-1})	65.6	37.6

from the results obtained in this work. Nevertheless, the fact that Lewatit formed practically no fines during the fluidization test indicates that the material should be very stable from a mechanical point of view when utilized in the proposed TSA process.

3.2 Modeling results

3.2.1 Adsorption equilibrium model

For further evaluation of the proposed TSA process, it is necessary to find a mathematical model that describes the adsorption properties of both materials at all relevant CO_2 partial pressures and operating temperatures. Therefore, an adsorption model was selected to mathematically describe the CO_2 adsorption behavior of both adsorbent materials. At first, the commonly known adsorption model of Langmuir (see Eqs. (1 and 2) in Sect. 2.3.1) was applied.

The parameters q_{max}, b_∞, and ΔH_{ADS} were fitted to the experimentally determined equilibrium adsorption isotherms by using the non-linear least square method. The resulting parameters are shown in Table 3.

For 13X, the Langmuir model already represented a good fit to the measured isotherms. For description of the CO_2 equilibrium adsorption behavior (isotherms) on Lewatit, the Langmuir model was, however, not sufficient to consistently describe the obtained adsorption data (see Fig. 7). Therefore, the adsorption model proposed by Toth (see Eqs. (3–6) in Sect. 2.3.1) was applied instead. This model was already proposed by Veneman et al. [35] for mathematical description of the CO_2 adsorption isotherms for Lewatit.

For the Toth model, also the parameters b_0, n_{S0}, χ, t_0, α, and ΔH were fitted to the measured equilibrium adsorption data by using the non-linear least square method. The reference temperature T_0 was taken as 343 K. The adsorption isotherms obtained with the Toth model were found to be suitable for both materials as can be seen in Figs. 7 and 8. The obtained model parameters for each material are displayed in Table 4. The error margin of the calculated CO_2 adsorption with the fitted Toth model is at ± 0.09 mol kg^{-1} for Lewatit and at ± 0.11 mol kg^{-1} for 13X (see Figs. 18 and 19). For Lewatit, the Toth model parameters by Sutanto et al. and Veneman et al. [35, 36] were compared to the own model parameters. The model parameters derived by Sutanto et al. are in a very close range to the values predicted in this work (see Fig. 7). The model by Veneman et al., however, clearly overpredicts the adsorption capacities measured in this work.

In order to validate the heat of adsorption from the derived Toth model and to gain information on the specific heat capacity (c_p) of the adsorbent materials, additional measurements in a combined TGA/DSC device (NETZSCH STA 409 PC Luxx®) have been performed. According to the approach by Toth, the heat of adsorption is dependent on the temperature and the loading of the sorbent materials (see Eq. (7)). DSC measurements have been performed at 50 and 95 °C with a stepwise increase of CO_2 concentration from 0 to 40%, balanced with N_2, to quantify the heat of adsorption in dependency of the CO_2 loading. The obtained ΔH_{ADS} data points from the DSC measurements are displayed in Figs. 20 and 21, together with the calculated ΔH isotherms resulting from Eq. (7). As can be seen from the figures, the calculated values for the heat of adsorption are in quite good agreement with the measured values. Furthermore, the heat capacities were measured for both materials during the conditioning phase before the adsorption measurements and were obtained with 1.58 kJ kg^{-1} K^{-1} for Lewatit and 0.93 kJ kg^{-1} K^{-1} for 13X. This is very well in line with the values reported by Veneman et al. (1.5 kJ kg^{-1} K^{-1} for Lewatit) [35] and Chue et al. (0.92 kJ kg^{-1} K^{-1} for 13X) [42].

3.2.2 TSA process simulations

The obtained Toth adsorption models were integrated in the previously described TSA process simulation tool, and process simulations were performed to evaluate the regeneration

Table 4 Toth isotherm parameters for own model fitting, compared to other model fittings for Lewatit by Sutanto et al. and Veneman et al.

Toth parameters	Lewatit	13X	Sutanto et al. [36]	Veneman et al. [35]
n_{s0} (mol kg^{-1})	3.13	19.0	3.7	3.4
χ (−)	0	0	0	0
T_0 (K)	343	343	353	353
b_0 (bar^{-1})	282	2.47	188.6	408.84
ΔH_0 (kJ mol^{-1})	106	61.7	111	86.7
t_0 (−)	0.34	0.30	0.3	0.3
α (−)	0.42	0.49	0.5	0.14

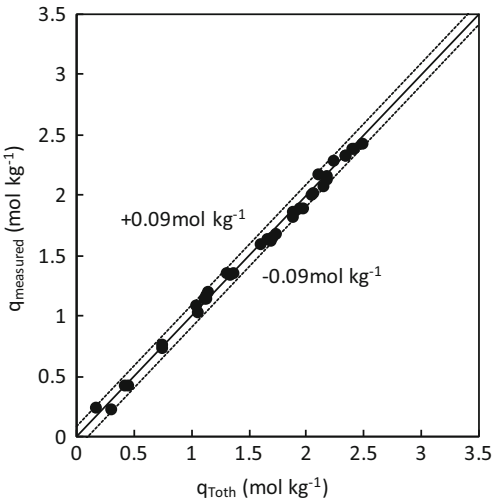

Fig. 18 Parity plot of CO_2 adsorption data measured in TGA and FB vs. calculated CO_2 adsorption with Toth model fitting for Lewatit

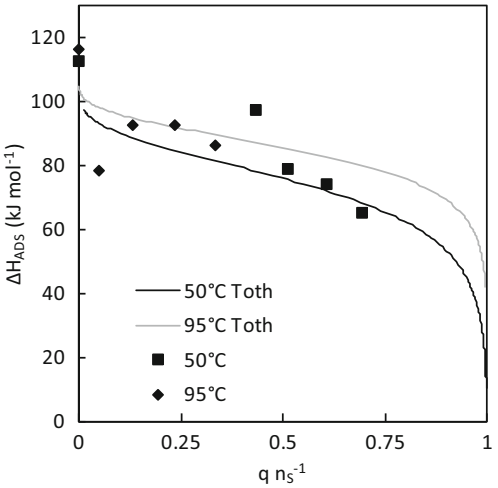

Fig. 20 ΔH_{ADS} measurements with DSC and calculated ΔH_{ADS} with Toth model for Lewatit

energy demand in the desorber for different operating conditions. The resulting specific regeneration energy demands for the different operating conditions studied are displayed in Figs. 22 and 23. It seems that the values obtained in this work are well in the range of the required energy requirements for other biogas upgrading technologies as reported by Patterson et al. and Sun et al. [43, 44]. However, the simplified model used in this study did not consider for any heat integration measures such as previously proposed by Pröll et al. [14], Vogtenhuber et al. [46], or Sutanto et al. [36]. Hence, one can expect that the specific regeneration energy demands derived in this work can be further reduced, if such measures are applied to the TSA process. Mainly due to its low heat of adsorption, 13X requires only about half of the energy input for regeneration of Lewatit, in case the same operating conditions are compared. However, according to the adsorbent regeneration tests performed in this work, the regeneration of 13X is much slower at low temperatures. This suggests that the desorber temperature in the TSA process needs to be higher than 95 °C in case 13X is used. In contrast to that, for Lewatit, the operating temperature of the desorber may need to be limited to about 90 °C due to a lack of thermal stability in the presence of air oxygen. Also, the regeneration energy demand generally increases by roughly 20–30% if the residual CO_2 content in the adsorber off-gas is reduced from 10 to 2%vol (Figs. 22 and 23).

As mentioned before, air was used as stripping gas for the biogas upgrading simulation, instead of steam, as proposed by Pröll et al. [14] for post-combustion CO_2 capture applications. This helps to reduce the energy demand of the TSA process significantly, in case the separated CO_2 is not required at concentrated form for further utilization. Besides that point, it is known from literature that the capacity of 13X is reduced dramatically when water is present in the adsorption process

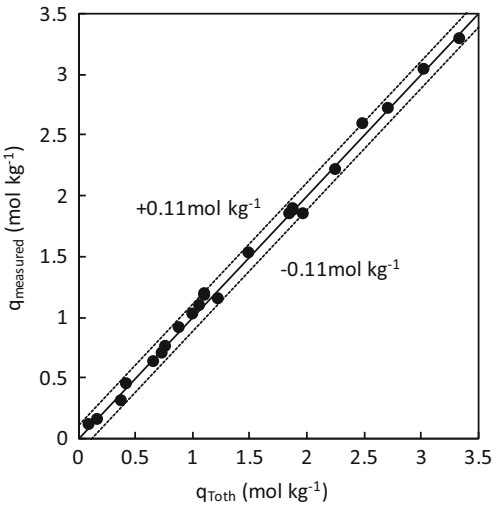

Fig. 19 Parity plot of CO_2 adsorption data measured in TGA and FB vs. calculated CO_2 adsorption with Toth model fitting for 13X

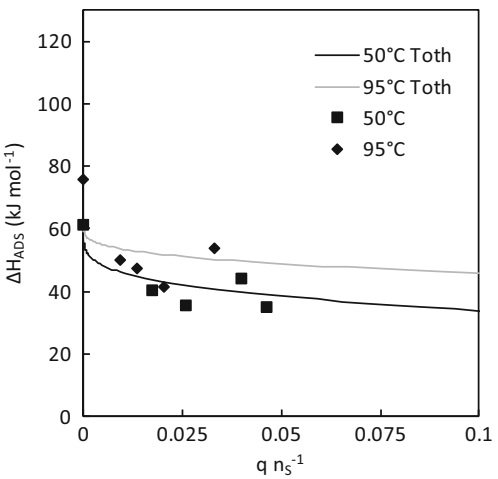

Fig. 21 ΔH_{ADS} measurements with DSC and calculated ΔH_{ADS} with Toth model for 13X

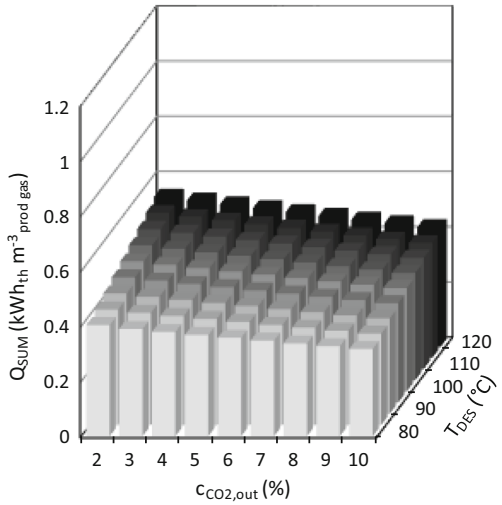

Fig. 22 Heating demand for regeneration of 13X, depending on regeneration temperature and biomethane quality

[45]. It is thus questionable if the TSA process could be operated without pre-drying step upstream to the adsorber in case 13X is used as adsorbent material. On the contrary, the CO_2 capture performance of Lewatit may even improve if water is present in the system [35]. Hence, the application of an amine functionalized adsorbent material may even allow for a simultaneous removal of various components (i.e., CO_2, H_2O, H_2S [47]) in a single apparatus. Also not considered in the simplified model used in this work are the methane recovery rates that can be expected from the process. However, from the methane adsorption properties obtained in this work, it can be expected that methane slip should be smaller or even eliminated completely in case Lewatit is used as adsorbent material.

While the intention of this work was to get a rough idea of the regeneration energy demand for further comparison of two different adsorbent materials, all of the abovementioned aspects need to be considered to get a clearer view on the techno-economic figures of the proposed TSA biogas upgrading process.

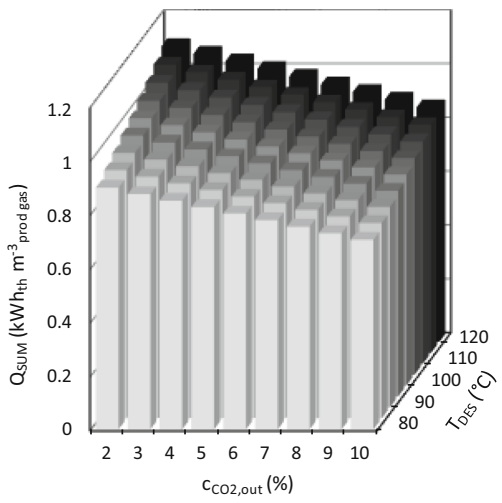

Fig. 23 Heating demand for regeneration of Lewatit, depending on regeneration temperature and biomethane quality

4 Conclusions

In this study, Lewatit® VP OC 1065 and Zeolite 13X have been evaluated for an application in a continuous TSA process for biogas upgrading. For this, the CO_2 adsorption isotherms, the adsorbent selectivities towards CO_2 adsorption, and the thermal and mechanical stability were measured for both materials. In a further step, the measured CO_2 adsorption isotherms of both materials were used to derive model parameters of a suitable mathematical adsorption model. The adsorption models were then incorporated into an existing simulation tool for the proposed multistage fluidized bed TSA process for continuous biogas upgrading. Based on the performed material assessment and the performed process simulations, the following conclusions can be drawn.

Both materials show a sufficiently high CO_2 adsorption capacity. 13X has a higher capacity for CO_2 partial pressures above 0.12 bar, whereas Lewatit shows higher capacities at pressures below 0.12 bar. On the other hand, at low partial pressures, Lewatit shows a high CO_2 capacity at practical adsorption temperatures as well as a low CO_2 capacity at the desired operating temperatures of the desorber.

Neither Lewatit nor 13X showed a significant CH_4 adsorption capacity, which indicates that a highly selective CO_2 removal from biogas should be possible with both adsorbent materials. This in turn means that it is possible to achieve high purities and methane recovery rates in a TSA process that is operated with either one of the two adsorbent materials.

13X shows no degradation at higher temperatures and is stable to temperatures of at least 190 °C. Lewatit started to degrade at 110 °C in N_2 atmosphere and even at 90 °C in air atmosphere. Consequently, it is concluded that the operating temperature and the solid residence time in the desorber of the TSA reactor need to be limited in order to avoid high make-up streams of Lewatit.

The mechanical stability of Lewatit is given, and no weight loss during fluidization was encountered. The tested 13X is not suitable for an application in a fluidized bed, as it showed high abrasion and breakage when it was fluidized.

In general, both materials showed to be promising adsorbents for utilization in a TSA biogas upgrading process. Nevertheless, the 13X-type adsorbent tested in this work is not recommended for the proposed process, operating in fluidized beds, due to its low mechanical stability, unless this property is enhanced.

The data obtained in the experimental part of this work was used to establish a mathematical adsorption model with the respective fitting parameters. The obtained Toth adsorption

models showed excellent alignment with the measured data and were further implemented to an existing process simulation model.

First, results from the process simulation with both materials revealed that 13X requires almost half of the energy for regeneration than Lewatit mainly because of the difference in their heat of adsorption. Nevertheless, for both adsorbent materials, the derived regeneration energy demands were well in the range of those reported for existing technologies if though the simplified process simulation tool used in this work did not account for any heat integration measures.

In a next step, further research will be dedicated to evaluate and quantify the benefits of different heat-integration measures to the process. In addition, co-adsorption of water and other species will be assessed for both materials and the corresponding impact on the process energy demand will be quantified. Furthermore, at least one of the adsorbent materials will be tested in continuous operation using an existing TSA bench-scale unit at TU Wien and raw biogas from a biogas facility in Austria.

Acknowledgments Open access funding provided by TU Wien (TUW).

Notation α, Toth parameter; b, Temperature dependent Langmuir / Toth parameter (bar^{-1}); b_∞. Langmuir parameter at infinite temperature (bar^{-1}); b_0, Toth parameter at reference temperature (bar^{-1}); χ Toth parameter; ΔH_{ADS}, Heat of adsorption Langmuir (J mol^{-1}); ΔH_0, Toth heat of adsorption at zero surface coverage (J mol^{-1}); n_s, Temperature dependent maximum Loading Toth (mol kg^{-1}); n_{s0}, Maximum loading Toth at reference temperature (mol kg^{-1}); p_{CO2}, Partial pressure of CO_2 (bar); q, Adsorption uptake (mol kg^{-1}); R, Universal gas constant (J $molK^{-1}$); Θ, Fractional loading (−); T_0, Reference temperature (K); T, Temperature (K); t, Temperature dependent Toth parameter; t_0, Toth parameter at reference temperature T_0; U_{mf}, Minimum fluidization velocity

Funding information This work was part of the Project bioCH4.0 funded by the Austrian Governments Climate and Energy (Fund No. 853612) coordinated by TU Wien. Financial support given by the Climate and Energy Fund is gratefully acknowledged.

References

1. Awe OW, Zhao Y, Nzihou A, Minh DP, Lyczko N (2017) A review of biogas utilisation, purification and upgrading technologies. Waste Biomass Valoriz 8(2):267–283. https://doi.org/10.1007/s12649-016-9826-4
2. Ryckebosch E, Drouillon M, Vervaeren H (2011) Techniques for transformation of biogas to biomethane. Biomass Bioenergy 35(5):1633–1645. https://doi.org/10.1016/j.biombioe.2011.02.033
3. Mayer T (2012) Über die Aufbereitung biogener Gase mittels adsorption. Dissertation, TU Wien
4. IEA-Bioenergy (2016) IEA Bioenergy Task 37 country reports summary 2015. doi: 978–1–910154-11-3
5. Makaruk A, Miltner M, Harasek M (2010) Membrane biogas upgrading processes for the production of natural gas substitute. Sep Purif Technol 74(1):83–92. https://doi.org/10.1016/j.seppur.2010.05.010
6. Santos MPS, Grande CA, Rodrigues AE (2011) Pressure swing adsorption for biogas upgrading, effect of recycling streams in pressure swing adsorption design. Ind Eng Chem Res 50(2):974–985. https://doi.org/10.1021/ie100757u
7. TU Wien (2012) Biogas to biomethane technology review. IEE project BioMethane Regions, Deliverable. Reference: Task 3.1.1
8. Petersson A, Wellinger A (2009) Biogas upgrading technologies—developments and innovations. IEA bioenergy, task 37—energy from biogas landfill gas
9. Svensson H, Edfeldt J, Zejnullahu Velasco V, Hulteberg C, Karlsson HT (2014) Solubility of carbon dioxide in mixtures of 2-amino-2-methyl-1-propanol and organic solvents. Int J Greenh Gas Control 27:247–254. https://doi.org/10.1016/j.ijggc.2014.06.004
10. Svensson H, Zejnullahu Velasco V, Hulteberg C, Karlsson HT (2014) Heat of absorption of carbon dioxide in mixtures of 2-amino-2-methyl-1-propanol and organic solvents. Int J Greenh Gas Control 30:1–8. https://doi.org/10.1016/j.ijggc.2014.08.022
11. Zhang W, Liu H, Sun C, Drage TC, Snape CE (2014) Performance of polyethyleneimine-silica adsorbent for post-combustion CO_2 capture in a bubbling fluidized bed. Chem Eng J 251:293–303. https://doi.org/10.1016/j.cej.2014.04.063
12. Yu Q, Delgado JDLP, Veneman R, Brilman DWF (2017) Stability of a benzyl amine based CO_2 capture adsorbent in view of regeneration strategies. Ind Eng Chem Res 56(12):3259–3269. https://doi.org/10.1021/acs.iecr.6b04645
13. Drage TC, Arenillas A, Smith KM, Snape CE (2008) Thermal stability of polyethylenimine based carbon dioxide adsorbents and its influence on selection of regeneration strategies. Microporous Mesoporous Mater 116(1-3):504–512. https://doi.org/10.1016/j.micromeso.2008.05.009
14. Pröll T, Schöny G, Sprachmann G, Hofbauer H (2016) Introduction and evaluation of a double loop staged fluidized bed system for post-combustion CO_2 capture using solid sorbents in a continuous temperature swing adsorption process. Chem Eng Sci 141:166–174. https://doi.org/10.1016/j.ces.2015.11.005
15. Schöny G, Zehetner E, Fuchs J, Pröll T, Sprachmann G, Hofbauer H (2016) Design of a bench scale unit for continuous CO_2 capture via temperature swing adsorption—fluid-dynamic feasibility study. Chem Eng Res Des 106:155–167. https://doi.org/10.1016/j.cherd.2015.12.018
16. Schöny G, Dietrich F, Fuchs J, Pröll T, Hofbauer H (2017) A multistage fluidized bed system for continuous CO_2 capture by means of temperature swing adsorption – first results from bench scale experiments. Powder Technol 316:519–527. https://doi.org/10.1016/j.powtec.2016.11.066
17. Choi S, Drese JH, Jones CW (2009) Adsorbent materials for carbon dioxide capture from large anthropogenic point sources. ChemSusChem 2(9):796–854. https://doi.org/10.1002/cssc.200900036
18. Vivio-Vilches JF, Pérez-Cadenas AF, Maldonado-Hódar FJ et al (2017) Biogas upgrading by selective adsorption onto CO_2 activated carbon from wood pellets. Journal of Environmental Chemical Engineering 5(2):1386–1393. https://doi.org/10.1016/j.jece.2017.02.015
19. Cavenati S, Grande CA, Rodrigues AE (2008) Metal organic framework adsorbent for biogas upgrading. Ind Eng Chem Res 47(16):6333–6335. https://doi.org/10.1021/ie8005269

20. Cavenati S, Grande CA, Rodrigues AE (2004) Adsorption equilibrium of methane, carbon dioxide, and nitrogen on zeolite 13X at high pressures. J Chem Eng Data 49(4):1095–1101. https://doi.org/10.1021/je0498917
21. Lee J-S, Kim J-H, Kim J-T, Suh JK, Lee JM, Lee CH (2002) Adsorption equilibria of CO_2 on zeolite 13X and zeolite X/activated carbon composite. J Chem Eng Data 47(5):1237–1242. https://doi.org/10.1021/je020050e
22. Li Y, Yi H, Tang X, Li F, Yuan Q (2013) Adsorption separation of CO_2/CH_4 gas mixture on the commercial zeolites at atmospheric pressure. Chem Eng J 229:50–56. https://doi.org/10.1016/j.cej.2013.05.101
23. Montanari T, Finocchio E, Salvatore E, Garuti G, Giordano A, Pistarino C, Busca G (2011) CO_2 separation and landfill biogas upgrading: a comparison of 4A and 13X zeolite adsorbents. Energy 36(1):314–319. https://doi.org/10.1016/j.energy.2010.10.038
24. Na B-K, Koo K-K, Eum H-M, Lee H, Song HK (2001) CO_2 recovery from flue gas by PSA process using activated carbon. Korean J Chem Eng 18(2):220–227. https://doi.org/10.1007/BF02698463
25. Siriwardane RV, Shen M-S, Fisher EP, Poston JA (2001) Adsorption of CO_2 on molecular sieves and activated carbon. Energy Fuel 15(2):279–284. https://doi.org/10.1021/ef000241s
26. Do D, Wang K (1998) A new model for the description of adsorption kinetics in heterogeneous activated carbon. Carbon N Y 36(10):1539–1554. https://doi.org/10.1016/S0008-6223(98)00145-6
27. Walton KS, Abney MB, LeVan MD (2006) CO_2 adsorption in Y and X zeolites modified by alkali metal cation exchange. Microporous Mesoporous Mater 91(1-3):78–84. https://doi.org/10.1016/j.micromeso.2005.11.02
28. International Zeolite Association (2016) IZA Structure Commission. http://www.iza-structure.org/databases/DatabaseHistory.htm. Accessed 10 Mar 2017
29. Veneman R, Li ZS, Hogendoorn J a et al (2012) Continuous CO_2 capture in a circulating fluidized bed using supported amine sorbents. Chem Eng J 207–208:18–26. https://doi.org/10.1016/j.cej.2012.06.100
30. Alesi WR, Kitchin JR (2012) Evaluation of a primary amine-functionalized ion-exchange resin for CO_2 capture. Ind Eng Chem Res 51(19):6907–6915. https://doi.org/10.1021/ie300452c
31. Gray ML, Hoffman JS, Hreha DC, Fauth DJ, Hedges SW, Champagne KJ, Pennline HW (2009) Parametric study of solid amine sorbents for the capture of carbon dioxide. Energy Fuel 23(10):4840–4844. https://doi.org/10.1021/ef9001204
32. Heydari-Gorji A, Sayari A (2012) Thermal, oxidative, and CO_2-induced degradation of supported polyethylenimine adsorbents. Ind Eng Chem Res 51(19):6887–6894. https://doi.org/10.1021/ie3003446
33. Tirio AP, Wagner R (2015) Process and apparatus for carbon dioxide and carbonyl sulfide capture via ion exchange resins. US Patent 9028590 B2
34. Veneman R, Hilbers T, Brilman DWF, Kersten SRA (2016) CO_2 capture in a continuous gas-solid trickle flow reactor. Chem Eng J 289:191–202. https://doi.org/10.1016/j.cej.2015.12.066
35. Veneman R, Frigka N, Zhao W, Li Z, Kersten S, Brilman W (2015) Adsorption of H_2O and CO_2 on supported amine sorbents. Int J Greenh Gas Control 41:268–275. https://doi.org/10.1016/j.ijggc.2015.07.014
36. Sutanto S, Dijkstra JW, Pieterse JAZ, Boon J, Hauwert P, Brilman DWF (2017) CO_2 removal from biogas with supported amine sorbents: first technical evaluation based on experimental data. Sep Purif Technol 184:12–25. https://doi.org/10.1016/j.seppur.2017.04.030
37. Do DD (1998) Adsorption analysis: equilibria and kinetics, series on. Imperial College Press, London
38. Wang Y, LeVan MD (2009) Adsorption equilibrium of carbon dioxide and water vapor on zeolites 5A and 13X and silica gel: pure components. J Chem Eng Data 54(10):2839–2844. https://doi.org/10.1021/je800900a
39. Belmabkhout Y, De Weireld G, Sayari A (2009) Amine-bearing mesoporous silica for CO_2 and H_2S removal from natural gas and biogas. Langmuir 25(23):13275–13278. https://doi.org/10.1021/la903238y
40. Mulgundmath VP, Tezel FH, Saatcioglu T, Golden TC (2011) Adsorption and separation of CO_2/N_2 and CO_2/CH_4 by 13X zeolite. Can J Chem Eng 90(3):730–738. https://doi.org/10.1002/cjce.20592
41. Hallenbeck AP, Kitchin JR (2013) Effects of O_2 and SO_2 on the capture capacity of a primary-amine based polymeric CO_2 sorbent. Ind Eng Chem Res 52(31):10788–10794. https://doi.org/10.1021/ie400582a
42. Chue KT, Kim JN, Yoo J et al (1995) Comparison of activated carbon and zeolite 13X for CO_2 recovery from flue gas by pressure swing adsorption. Ind Eng Chem Res 34(2):591–598. https://doi.org/10.1021/ie00041a020
43. Patterson T, Esteves S, Dinsdale R, Guwy A (2011) An evaluation of the policy and techno-economic factors affecting the potential for biogas upgrading for transport fuel use in the UK. Energy Policy 39(3):1806–1816. https://doi.org/10.1016/j.enpol.2011.01.017
44. Sun Q, Li H, Yan J, Liu L, Yu Z, Yu X (2015) Selection of appropriate biogas upgrading technology-a review of biogas cleaning, upgrading and utilisation. Renew Sust Energ Rev 51:521–532. https://doi.org/10.1016/j.rser.2015.06.029
45. Wang Y, LeVan MD (2010) Adsorption equilibrium of binary mixtures of carbon dioxide and water vapor on zeolites 5A and 13X. J Chem Eng Data 55(9):3189–3195. https://doi.org/10.1021/je100053g
46. Vogtenhuber H, Hofmann R, Schöny G et al (2017) Development of an efficient heat balance concept for a TSA-process considering heat-pump integration. Proceedings of the 10th international conference on sustainable energy and environmental protection, University of Maribor 1-12. ISBN: 978-961-286-061
47. Belmabkhout Y, Heymans N, Weireld GD, Sayari A (2011) Simultaneous adsorption of H_2S and CO_2 on Triamine-grafted pore-expanded mesoporous MCM-41 silica. Energy Fuel 25(3):1310–1315. https://doi.org/10.1021/ef1015704